SUPPLEMENTAL MATERIAL

tRNA-like leader-trailer interaction promotes 3′-end maturation of MALAT1

Seyed-Fakhreddin Torabi[1,2], Suzanne J. DeGregorio[1,2], and Joan A. Steitz[1,2]

[1]Department of Molecular Biophysics and Biochemistry, Yale University, New Haven, CT 06536, USA.

[2]Howard Hughes Medical Institute, Yale University School of Medicine, New Haven, CT 06536, USA.

Corresponding authors: seyed.torabi@yale.edu, joan.steitz@yale.edu

This file includes:

Supplemental Figures S1, S2, S3, S4, S5, S6, S7 and S8

Supplemental References

SUPPLEMENTAL FIGURES

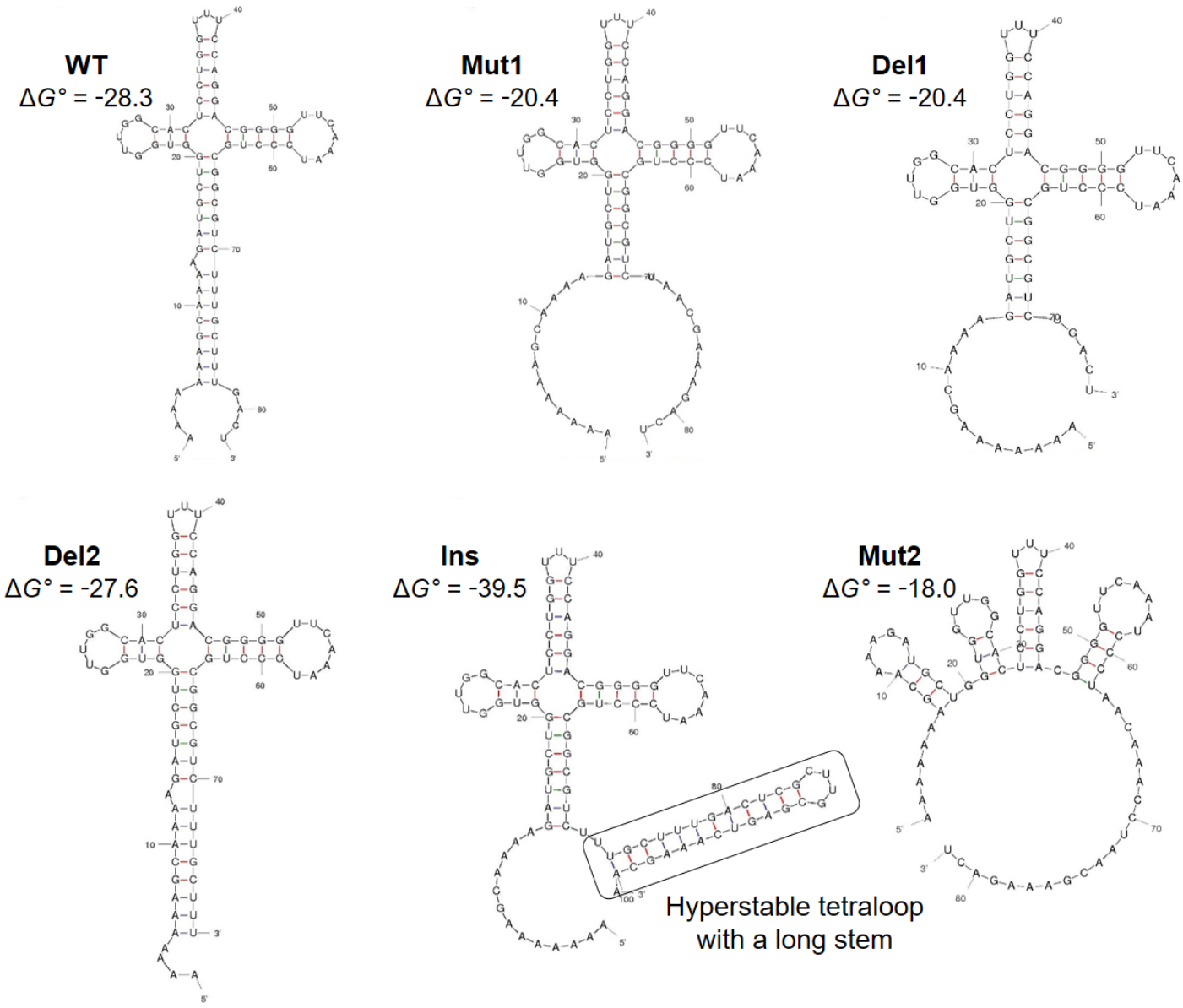

Figure S1. Predicted secondary structures, obtained by Mfold (Zuker 2003), formed by mascRNAs including the upstream MALAT1 A-rich tract and the downstream 3′ trailer sequence in the various RNA constructs tested in Figure 1 and 3. In Mut1, Del1, Ins and Mut2, the base-pairing interaction between the MALAT1 A-rich tract and the mascRNA 3′-trailer sequence is disrupted. In Ins, a hyperstable tetraloop (Chen and Garcia 2013) introduced downstream of the mascRNA 3′ trailer sequesters the 3′ trailer sequence. Calculated ΔG° values are in kcal/mol at 37°C.

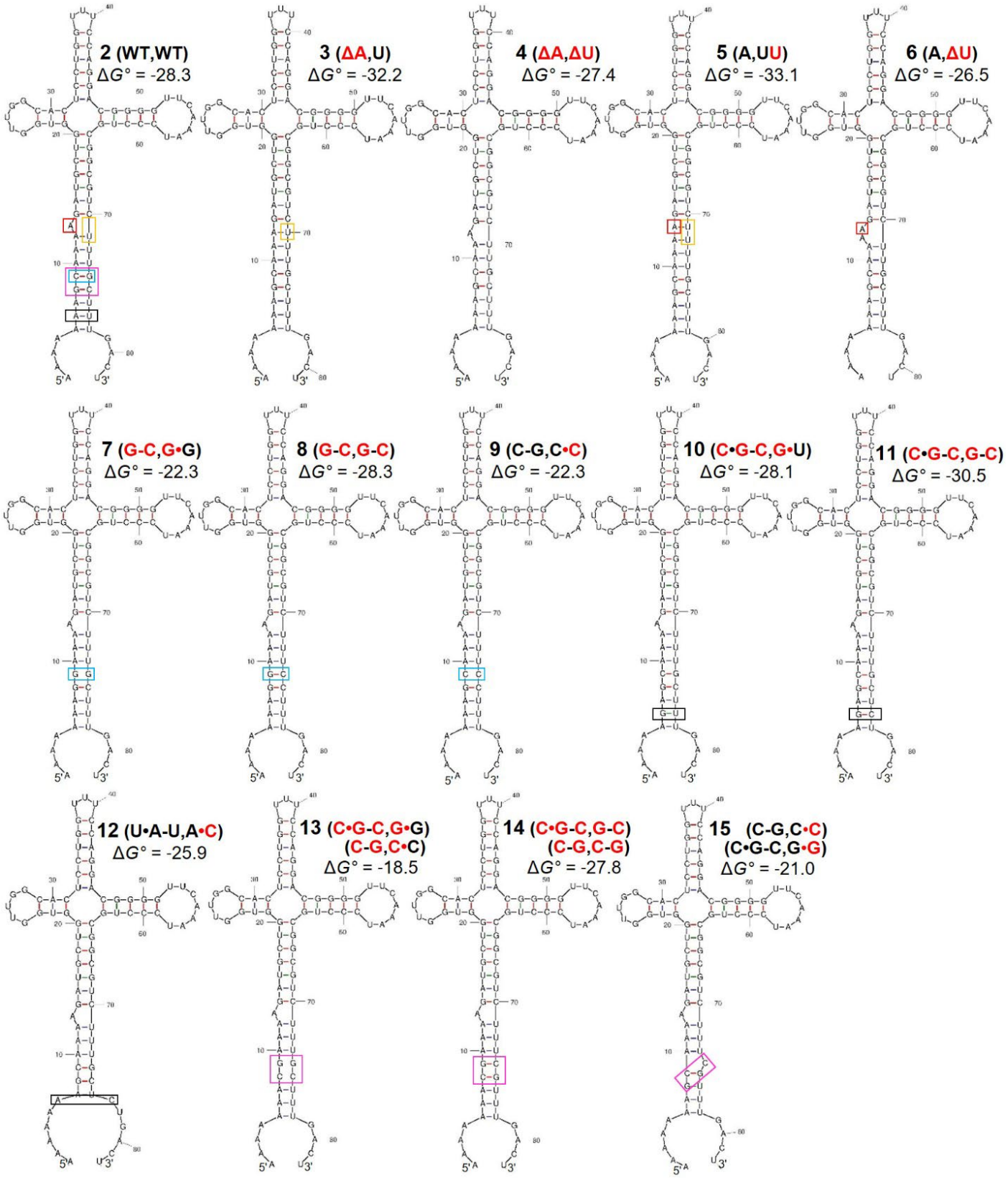

Figure S2. Predicted secondary structures of the mascRNAs, obtained by Mfold (Zuker 2003), including their upstream MALAT1 A-rich tracts and downstream 3′-trailer sequences, in various RNA constructs tested in Figure 2. Boxed nucleotides designate the regions mutated as shown in Figure 2A and B. Calculated ΔG° values are in kcal/mol at 37°C.

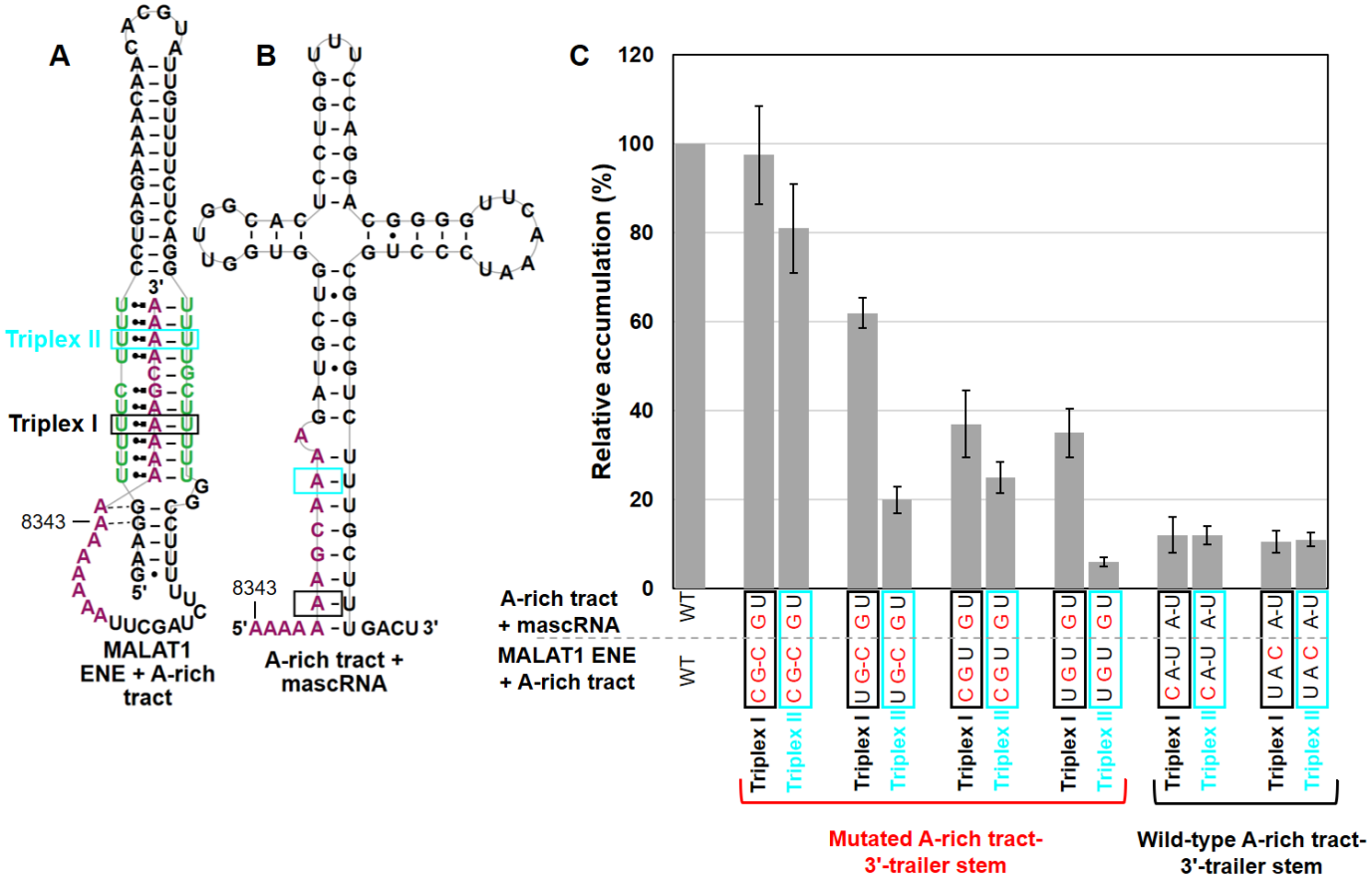

Figure S3. The effects of mutating U•A-U triple bases in the MALAT1 triplex I or triplex II region on the stability and accumulation of the β-globin reporter mRNA. (A) Schematic diagram of the triple helical structure of the MALAT1 ENE. (B) Predicted secondary structure of the mascRNA including the base-pairing interaction between the MALAT1 A-rich tract and the mascRNA 3′-trailer sequence. Black and cyan boxes represent a single U•A-U mutated in the MALAT1 triplex I or triplex II, respectively, (A) or the mascRNA extended acceptor stem (B). (C) Quantification of the Northern blot analyses of intronless β-globin reporters containing different MALAT1 triplex mutants. Accumulation of the wild-type MALAT1, first bar on left, was set at 100%. Each pair of bars then compares the effect of the mutation on reporter accumulation when it is in triplex I or triplex II. Mutations that disrupt the base-pairing interaction between the MALAT1 A-rich tract and the mascRNA 3′-trailer sequence have more dramatic effects on the accumulation of the reporter if they are located in the triplex II region. Those mutations that maintain the wild-type base-pairing interactions between the A-rich tract and mascRNA 3′ trailer, the last two pairs on right, show the same reporter accumulation. These data are replotted and re-organized from a previous study (Figure 2B in (Brown et al. 2012)).

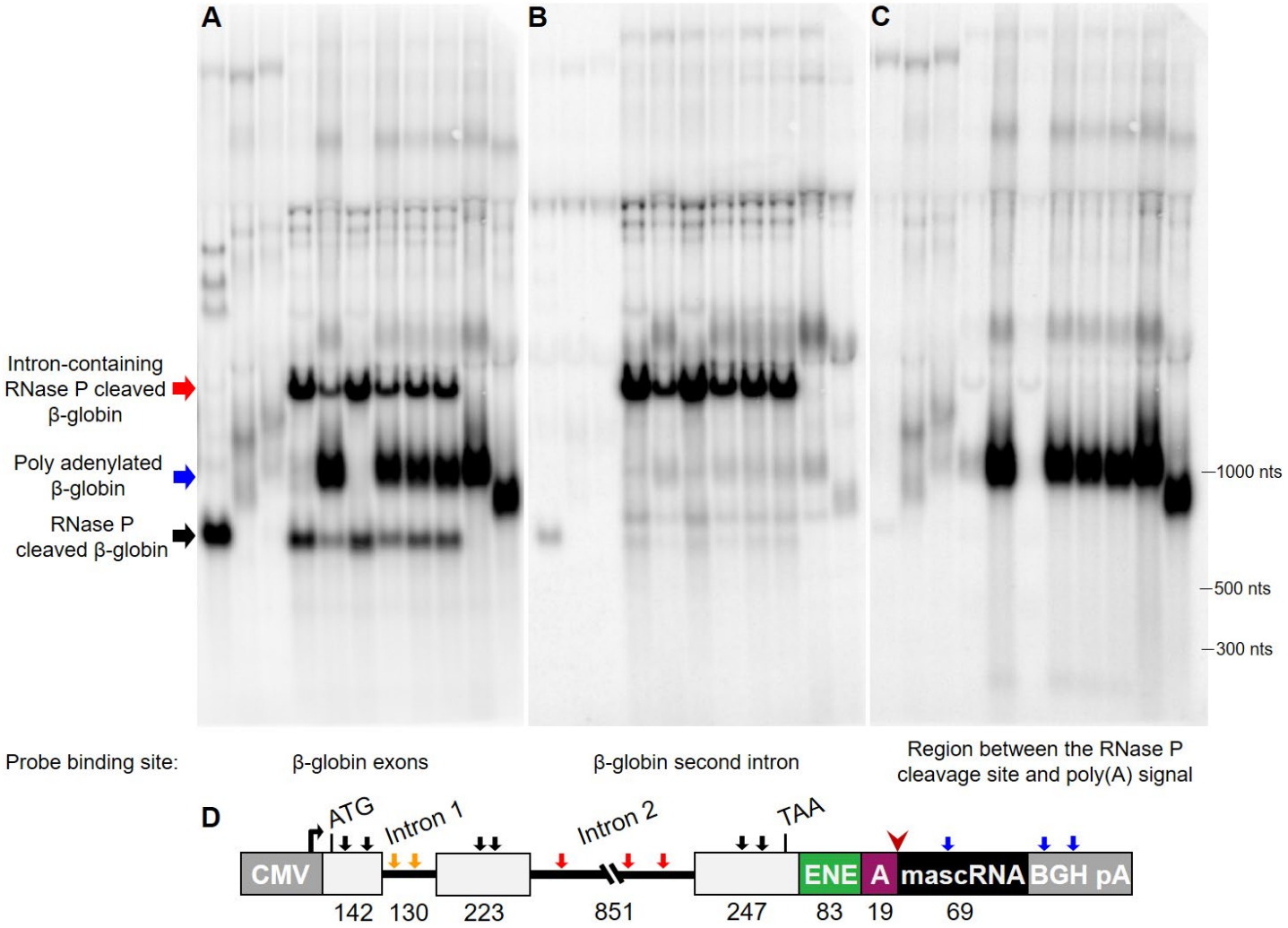

Figure S4. Northern blot analyses of representative blots shown in Figure 3 examined using probes targeting different regions of the β-WT reporter transcript: β-globin exons (A), the β-globin second intron (B) and a region between the RNase P cleavage site and the BGH poly(A) signal (C). DNA oligonucleotides targeting the first intron did not detect any of the transcripts identified by other probes. (D) Schematic of the intron-containing β-globin reporter construct (from Figure 3A) including more detail. The RNase P cleavage site is marked by an arrowhead. Binding sites for different probes used in Northern blot analyses (see Materials and Methods) are marked by colored arrows as in (A): black for β-globin exons, orange for the β-globin first intron, red for the β-globin second intron and blue for the region between the RNase P cleavage site and the poly(A) signal. Lengths (in nts) of different regions are given below.

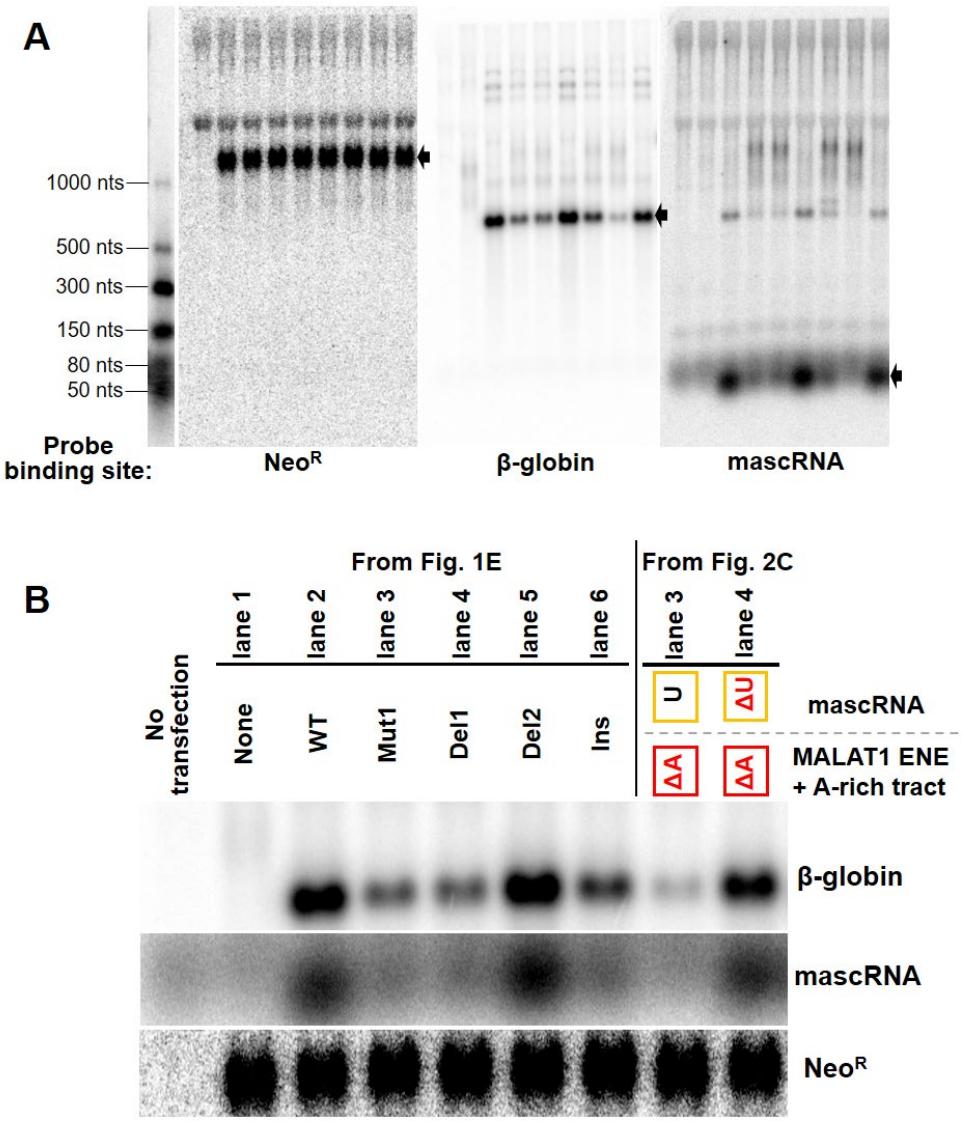

Figure S5. Accumulation of the β-globin reporter transcript changes proportionally with changes in the level of mascRNA produced from the reporter. (A) Uncropped images of Northern blots from Figure 1. The last two lanes are ΔA and ΔA-ΔU mutants. Blots probed for Neo^R, β-globin and mascRNA sequences. RNA moieties from the Low Range ssRNA ladder (NEB) are indicated on the left side. The black arrow on the right side of each image indicates the mobility of the RNA target anticipated for each probe. (B) Cropped Northern blot images showing β-globin, mascRNA transcripts and Neo^R bands. Lanes are marked as in Figure 1E and 2C.

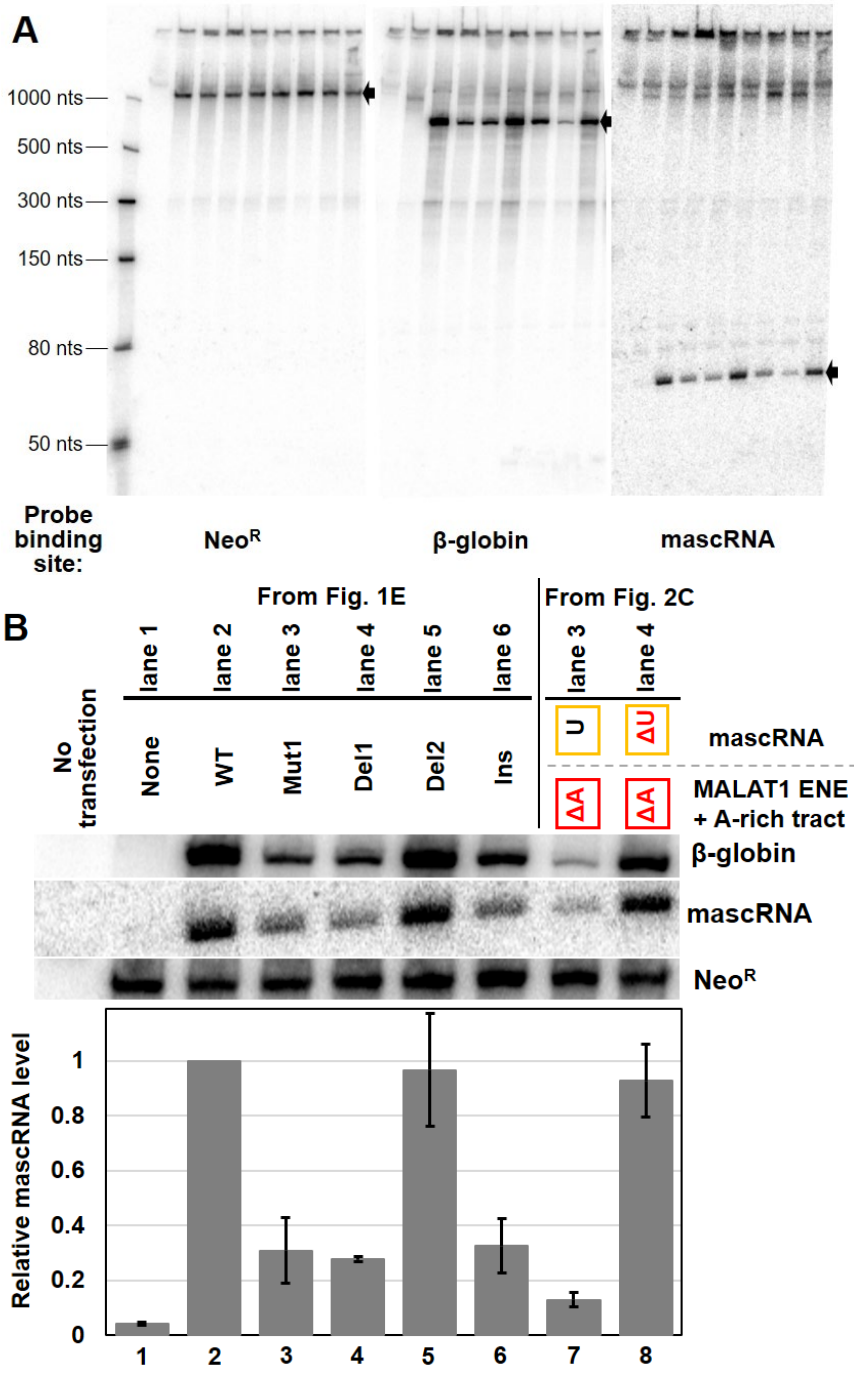

Figure S6. The base-pairing interactions between the A-rich tract and the mascRNA 3′ trailer and formation of a bulged nucleotide upstream of the RNase P cleavage site are required for robust RNase P cleavage activity and accumulation of mascRNA. (A) Uncropped Northern blot images of the same constructs shown in Supplemental Figure S5 using probes targeting Neo^R, β-globin and mascRNA transcripts. RNA transcripts are resolved on a gradient urea PAGE (4.5% on top and 12% on the bottom) to obtain sharp bands for mascRNA. The Low Range ssRNA ladder (NEB) bands are marked on the left side. Desired RNA target that is probed for is indicated by a black arrow on the right side of the image. (B) Northern blot analysis of β-globin, mascRNA and Neo^R transcripts (top) and quantitation (bottom) were carried out as in Figure 1E. Level of mascRNA from the wild-type construct is set at 1. Relative mascRNA level was the average of at least two independent experiments ± SD.

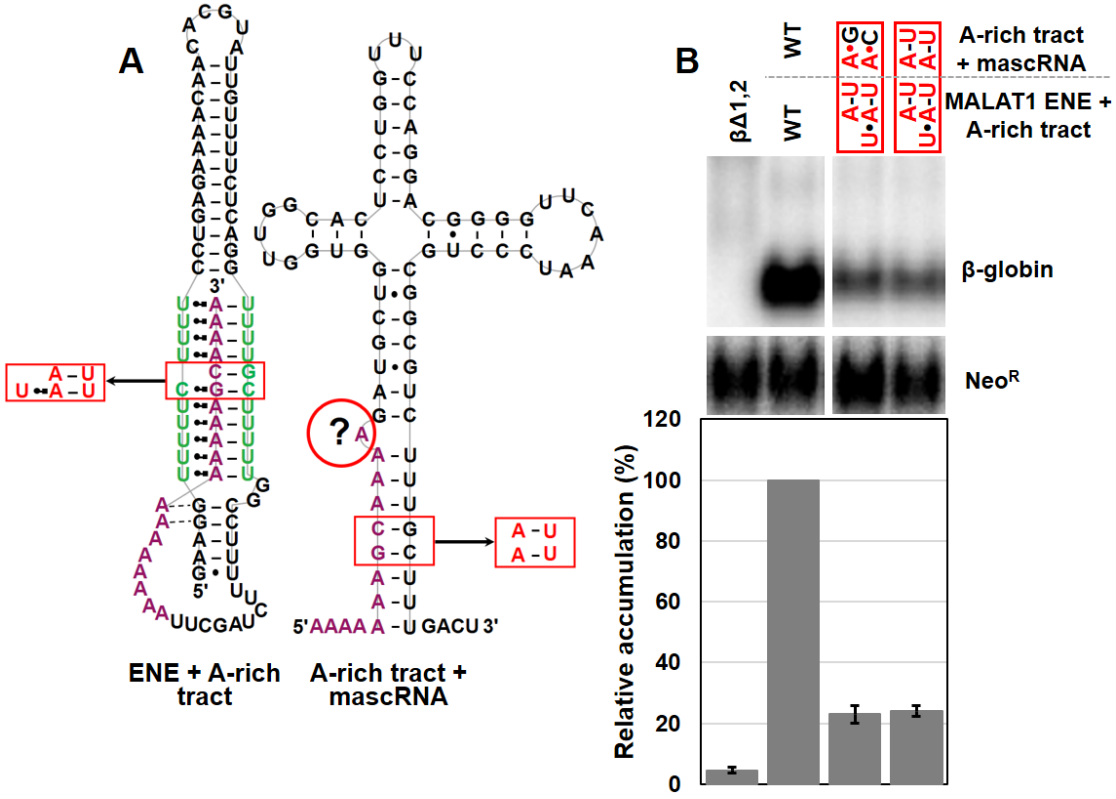

Figure S7. The GC dinucleotides in the wild-type A-rich tract are needed for its precise alignment with the mascRNA 3′ trailer. (A) Schematic diagram of the triple helical structure of the all U/A MALAT1 ENE and secondary structure of the mascRNA containing compensatory mutations in its 3′ trailer to maintain base-pairing interaction between the A-rich tract and the mascRNA 3′-trailer sequence. Without the GC dinucleotides in the A-rich tract and 3′ trailer, respectively, formation of a bulged nucleotide (circled in red) cannot be forced. (B) Northern blot analysis of β-globin and Neo^R transcripts (top) and its quantitation (bottom).

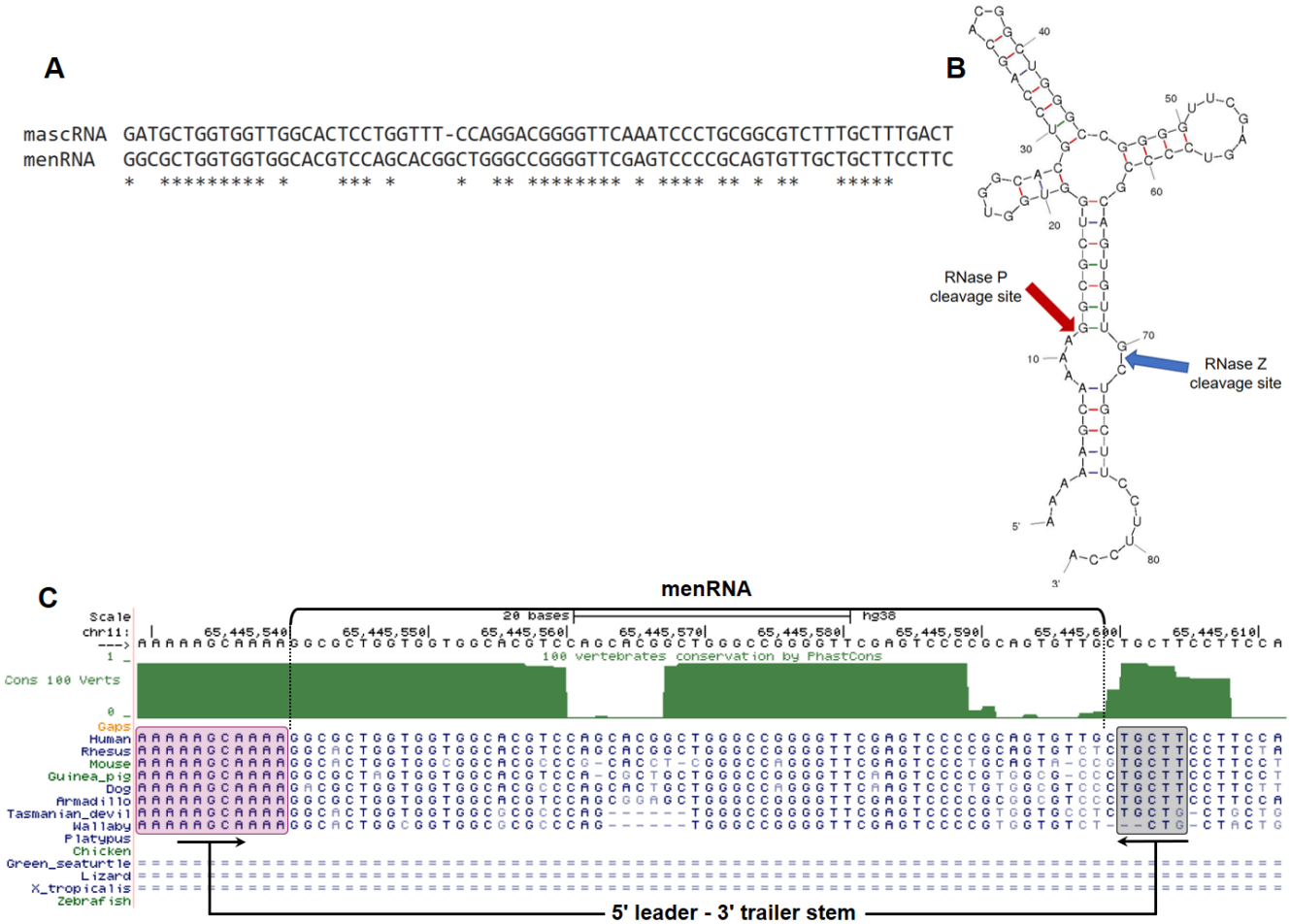

Figure S8. The human menRNA transcript is predicted to form a tRNA-like secondary structure with an extended acceptor stem in a fashion similar to the mascRNA. (A) Sequence alignment of the human mascRNA and menRNA. (B) Predicted secondary structure of the human menRNA showing the cleavage sites for RNase P and RNase Z. (C) Similar to the mascRNA, the 3′ trailers of menRNA homologs contain several nucleotides (boxed in black) that are highly conserved among vertebrates and can form base-paring interactions with the upstream MENβ A-rich tract.

SUPPLEMENTAL REFERENCES

Brown JA, Valenstein ML, Yario TA, Tycowski KT, Steitz JA. 2012. Formation of triple-helical structures by the 3'-end sequences of MALAT1 and MENbeta noncoding RNAs. *Proc Natl Acad Sci U S A* **109**: 19202-19207.

Chen AA, Garcia AE. 2013. High-resolution reversible folding of hyperstable RNA tetraloops using molecular dynamics simulations. *Proc Natl Acad Sci U S A* **110**: 16820-16825.

Zuker M. 2003. Mfold web server for nucleic acid folding and hybridization prediction. *Nucleic Acids Res* **31**: 3406-3415.